

The spin-triplet superconductivity induced by the charge fluctuation in extended Hubbard model

Seiichiro Onari^{1*}, Ryotaro Arita^{1,2}, Kazuhiko Kuroki³, and Hideo Aoki¹

¹Department of Physics, University of Tokyo, Hongo, Tokyo 113-0033, Japan

²Max-Planck-Institut für Festkörperforschung, Stuttgart, Germany

³Department of Applied Physics and Chemistry, University of Electro-Communications, Chofu, Tokyo 182-8585, Japan

(December 2, 2024)

The pairing symmetry in the electron mechanism for superconductivity is explored when charge fluctuations coexist with spin fluctuations. The extended Hubbard model is adopted to obtain, with the fluctuation exchange approximation, a phase diagram against the on-site Coulomb repulsion U and the off-site repulsion V for the square lattice with second-neighbor hopping t' . We have found that (i) for large $U (> 9)$ a triplet superconductivity with a $\sin(k_x + k_y)$ symmetry can appear just below the charge density wave phase. The pairing is degenerate with $\sin(k_x - k_y)$, so a chiral $\sin(k_x + k_y) + i \sin(k_x - k_y)$ that breaks the time reversal symmetry should result, which is a candidate for the gap function on the γ band of Sr_2RuO_4 and is consistent with a recent measurement of the specific heat. (ii) By systematically deforming the Fermi surface with varied t' , we have identified the region where the triplet pairing is most favored to be the region where the Fermi surface traverses the van Hove singularity with the charge susceptibility strongly enhanced.

PACS numbers: 74.20.Mn

I. INTRODUCTION

Spin-triplet superconductivity, which is arousing much interests in recent years, is fascinating in a number of ways. Theoretically, a most intriguing question is the following: if we consider the electron mechanism of superconductivity in the most frequently adopted Hubbard model with an on-site electron-electron repulsion, we can show that triplet superconductivity is very difficult to realize for the simple reason that the pairing interaction mediated by spin fluctuations is only $1/3$ in the triplet channel than in the singlet channel^{1,2}. So any theory attempting to explain triplet pairing has to overcome this question.

Experimentally, the discovery of superconductivity by Maeno and coworkers in the layered perovskite ruthenium oxide Sr_2RuO_4 have kicked off renewed interests. Suggestions for a triplet pairing in this material came from NMR Knight shift^{3,4} and polarized neutron scattering⁵. A broken time reversal symmetry is further observed with μSR ^{6,7} and small-angle neutron scattering⁸. As for the pairing symmetry, NMR and NQR relaxation rates have shown an absence of the Hebel-Slichter peak^{9,10}, which suggests line node(s) in the gap function, which was supported by a specific heat measurement¹¹. While the angular dependence of thermal conductivity indicates the presence of horizontal line-nodes¹², a recent field-orientation dependence of the specific heat shows that the gap in the active γ band has minima along [100] directions with the passive α and β bands having gap minima along [110] directions¹³.

A theoretical work by Zhitomirsky and Rice¹⁴ has proposed horizontal line nodes with a good fit to the specific heat measurement¹¹. As for the mechanism that sta-

bilizes triplet pairing, Kuwabara and Ogata¹⁵, and independently Sato and Kohmoto¹⁶, have suggested that triplet p -wave pairing can be induced by an anisotropy in the spin fluctuation. Kuwabara and Ogata¹⁵ have identified the most suitable gap function to be $\sin k_x + i \sin k_y$ that breaks the time-reversal symmetry, which was also proposed by Miyake and Narikiyo¹⁷. The chiral $\phi_x(k) + i\phi_y(k)$ ($\phi_x(k), \phi_y(k)$: p -wave like) has also been obtained with a third-order perturbation theory by Nomura and Yamada^{18,19} and more recently by Yanase and Ogata²⁰, and with the fluctuation exchange approximation (FLEX) for quasi-one-dimensional α and β bands by Kuroki *et al.*²¹.

However, the validity of perturbation results truncated at finite orders has to be checked by non-perturbative methods. Indeed, a recent quantum Monte Carlo (QMC) result by Kuroki *et al.* have shown that the singlet d -pairing dominates over the triplet for the γ band.²² This situation has led Arita *et al.* to show, with the dynamical cluster approximation (DCA), that $d_{x^2-y^2}$ pairing actually dominates over p -wave pairings as far as the on-site Hubbard model is concerned, while if we go over to the extended Hubbard model with off-site repulsion the triplet superconductivity can be favored but not dominant in extended Hubbard model employing nearest neighbor Coulomb repulsion for γ band in Sr_2RuO_4 .²³

Generally, there is a FLEX result by Arita *et al*¹ who show that triplet superconductivity is much weaker than singlet pairs for the one-band, on-site Hubbard model, which agrees with a phenomenology², while if charge fluctuations are enhanced by off-site repulsions triplet pairs have a chance to dominate. We have already shown triplet superconductivity can be dominant near the charge density wave (CDW) phase on square lattice with the FLEX in the extended Hubbard model.²⁴

So the purpose of this paper is to examine how triplet superconductivity can become dominant in the extended Hubbard model with the FLEX in general, and for γ band of Sr_2RuO_4 in particular. The extended Hubbard model has been studied, primarily for specific charge densities n , e.g., half-filling or quarter filling, by means of the quantum Monte Carlo method²⁵, the weak coupling theory²⁶, the mean-field approximation^{27,28}, the second-order perturbation²⁹, the random phase approximation³⁰, the FLEX approximation³¹, the slave-boson technique³², the bosonization and the renormalization group^{33,34}. Here we adopt the FLEX developed by Bickers *et al.*^{35–38}, which is a renormalized perturbation method to study pairing instabilities when exchange of spin and charge fluctuations are considered as dominant diagrams. This approximation is useful to explore the tendencies of dominant pairing relatively when the parameters are systematically varied. However, including the off-site Coulomb repulsion V susceptibilities and effective interactions become $(Z+1) \times (Z+1)$ matrices for the lattice coordination number Z ($= 4$ for the square lattice), which demand extremely computer resources. We show as far as the present finite-temperature result is concerned that (i) triplet $\sin(k_x + k_y)$ pairing appears in between singlet $\cos 2k_x - \cos 2k_y$ and the CDW phase for $U > 9$, and (ii) the pairing symmetry changes as $d_{x^2-y^2} \rightarrow \sin(k_x + k_y) \rightarrow \cos 2k_x - \cos 2k_y$ when the shape of the Fermi surface is varied by the second-neighbor hopping t' . Physically, all the results can be well explained by the structure and peak value of spin and charge susceptibilities.

II. FORMULATION

Let us start with the extended Hubbard Hamiltonian,

$$\mathcal{H} = - \sum_{i,j}^{\text{nn}, \text{nnn}} \sum_{\sigma} t_{ij} c_{i\sigma}^{\dagger} c_{j\sigma} + U \sum_i n_{i\uparrow} n_{i\downarrow} + \frac{1}{2} \sum_{i,j}^{\text{nn}} \sum_{\sigma\sigma'} V_{ij} n_{i\sigma} n_{j\sigma'}, \quad (1)$$

in the standard notation on a tetragonal lattice depicted in Fig.1, where nn (nnn) denotes nearest neighbor (next-nearest neighbor) sites. For the square lattice the unit of energy is taken to be the nearest-neighbor $t_{ij} = 1.0$, and lattice constant $a = 1$.

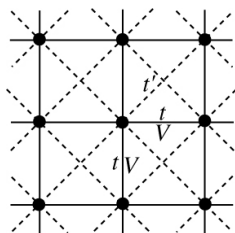


FIG. 1. A square lattice with nearest-neighbor hopping t and second neighbor hopping t' with the on-site Coulomb repulsion U and the nearest-neighbor repulsion V

To determine the dominant gap function, we solve Éliashberg's equation with the FLEX approximation,

$$\lambda \phi(k) = - \frac{T}{N} \sum_{k'} \Gamma(k, k') G(k') G(-k') \phi(k'), \quad (2)$$

where ϕ is the gap function, G Green's function, and Γ the pairing interaction with $k \equiv (\mathbf{k}, \omega_n)$. The eigenvalue λ , a measure of the pairing, becomes unity at $T = T_C$. For the calculation we take an $N = 32 \times 32$ lattice, the temperature $T = 0.03$, and the Matsubara frequency for fermions $-(2N_c - 1)\pi T \leq \omega_n \leq (2N_c - 1)\pi T$ with $N_c = 1024$.

Esirgen *et al.*^{31,39,40} have extended the FLEX method to general lattice Hamiltonians including the extended Hubbard model. Following them we introduce the pairing interaction,

$$\Gamma_s(k, k') = \sum_{\Delta\mathbf{r}, \Delta\mathbf{r}'} \{ \frac{3}{2} [V_{\text{sp}} \chi_{\text{sp}} V_{\text{sp}}] (k - k'; \Delta\mathbf{r}; \Delta\mathbf{r}') e^{i(\mathbf{k} \cdot \Delta\mathbf{r} + \mathbf{k}' \cdot \Delta\mathbf{r}')} - \frac{1}{2} [V_{\text{ch}} \chi_{\text{ch}} V_{\text{ch}}] (k - k'; \Delta\mathbf{r}; \Delta\mathbf{r}') e^{i(\mathbf{k} \cdot \Delta\mathbf{r} + \mathbf{k}' \cdot \Delta\mathbf{r}')} + \frac{1}{2} V_s(0; \Delta\mathbf{r}; \Delta\mathbf{r}') e^{i(\mathbf{k} \cdot \Delta\mathbf{r}' - \mathbf{k}' \cdot \Delta\mathbf{r})} \}, \quad (3)$$

for singlet pairing, and

$$\Gamma_t(k, k') = \sum_{\Delta\mathbf{r}, \Delta\mathbf{r}'} \{ -\frac{1}{2} [V_{\text{sp}} \chi_{\text{sp}} V_{\text{sp}}] (k - k'; \Delta\mathbf{r}; \Delta\mathbf{r}') e^{i(\mathbf{k} \cdot \Delta\mathbf{r} + \mathbf{k}' \cdot \Delta\mathbf{r}')} - \frac{1}{2} [V_{\text{ch}} \chi_{\text{ch}} V_{\text{ch}}] (k - k'; \Delta\mathbf{r}; \Delta\mathbf{r}') e^{i(\mathbf{k} \cdot \Delta\mathbf{r} + \mathbf{k}' \cdot \Delta\mathbf{r}')} + \frac{1}{2} V_t(0; \Delta\mathbf{r}; \Delta\mathbf{r}') e^{i(\mathbf{k} \cdot \Delta\mathbf{r}' - \mathbf{k}' \cdot \Delta\mathbf{r})} \}, \quad (4)$$

for triplet pairing. Here $\Delta\mathbf{r} (= \mathbf{0}, \pm\hat{x}, \pm\hat{y})$ is null or nearest-neighbor vectors,

$$\chi_{\text{sp}} = \bar{\chi} / (1 + V_{\text{sp}} \bar{\chi}), \quad \chi_{\text{ch}} = \bar{\chi} / (1 + V_{\text{ch}} \bar{\chi})$$

are the spin and charge susceptibilities, respectively, where $\bar{\chi}$ is the irreducible susceptibility,

$$\bar{\chi}(q; \Delta\mathbf{r}; \Delta\mathbf{r}') = - \frac{T}{N} \sum_{k'} e^{i\mathbf{k}' \cdot (\Delta\mathbf{r} - \Delta\mathbf{r}')} G(k' + q) G(k'), \quad (5)$$

and $V_{\text{ch}}(V_{\text{sp}})$ is the coupling between density (magnetic) fluctuations,

$$V_{\text{ch}}(q; \Delta\mathbf{r}; \Delta\mathbf{r}') = \begin{cases} U + 4[V_x \cos(q_x) + V_y \cos(q_y)], & \Delta\mathbf{r} = \Delta\mathbf{r}' = \mathbf{0}, \\ -V_x, & \Delta\mathbf{r} = \Delta\mathbf{r}' = \pm\hat{x}, \\ -V_y, & \Delta\mathbf{r} = \Delta\mathbf{r}' = \pm\hat{y} \end{cases} \quad (6)$$

$$V_{\text{sp}}(q; \Delta\mathbf{r}; \Delta\mathbf{r}') = \begin{cases} -U, & \Delta\mathbf{r} = \Delta\mathbf{r}' = \mathbf{0}, \\ -V_x, & \Delta\mathbf{r} = \Delta\mathbf{r}' = \pm\hat{x}, \\ -V_y, & \Delta\mathbf{r} = \Delta\mathbf{r}' = \pm\hat{y}, \end{cases} \quad (7)$$

where $q \equiv (\mathbf{q}, \epsilon_n)$ with $\epsilon_n = 2n\pi T$ being the Matsubara frequencies for bosons, and $V_x = V_y = V$ here. We have found that the q dependence of V_{sp} and V_{ch} does not significantly affect Γ_s and Γ_t . Accordingly the peak position of χ_{ch} is almost the same as that for $V_{\text{ch}}\chi_{\text{ch}}V_{\text{ch}}$ term in the expression for Γ .

$V_s(0; \Delta\mathbf{r}; \Delta\mathbf{r}')$, $V_t(0; \Delta\mathbf{r}; \Delta\mathbf{r}')$, appearing in the last lines in eqs.(3,4) respectively, are constant terms involving U and V ,

$$V_s(\mathbf{q}; \Delta\mathbf{r}; \Delta\mathbf{r}') = \begin{cases} 2U, & \Delta\mathbf{r} = \Delta\mathbf{r}' = \mathbf{0}, \\ V_x, & \Delta\mathbf{r} = \Delta\mathbf{r}' = \pm\hat{\mathbf{x}} \\ V_x e^{\pm iq_x}, & \Delta\mathbf{r} = -\Delta\mathbf{r}' = \pm\hat{\mathbf{x}} \\ V_y, & \Delta\mathbf{r} = \Delta\mathbf{r}' = \pm\hat{\mathbf{y}} \\ V_y e^{\pm iq_y}, & \Delta\mathbf{r} = -\Delta\mathbf{r}' = \pm\hat{\mathbf{y}} \end{cases} \quad (8)$$

$$V_t(\mathbf{q}; \Delta\mathbf{r}; \Delta\mathbf{r}') = \begin{cases} V_x, & \Delta\mathbf{r} = \Delta\mathbf{r}' = \pm\hat{\mathbf{x}} \\ -V_x e^{\pm iq_x}, & \Delta\mathbf{r} = -\Delta\mathbf{r}' = \pm\hat{\mathbf{x}} \\ V_y, & \Delta\mathbf{r} = \Delta\mathbf{r}' = \pm\hat{\mathbf{y}} \\ -V_y e^{\pm iq_y}, & \Delta\mathbf{r} = -\Delta\mathbf{r}' = \pm\hat{\mathbf{y}} \end{cases} \quad (9)$$

When the off-site interaction V is introduced all the vertices (V_{sp} , V_{ch} , V_s , V_t) as well as the susceptibilities become $(Z+1) \times (Z+1)$ matrices for the lattice coordination number Z ($= 4$ for the square lattice).

III. RESULT

A. A case study for Sr_2RuO_4

We consider γ band of Sr_2RuO_4 whose band filling is $n = 4/3$. To represent the shape of the Fermi surface obtained by ARPES⁴¹, we choose parameters $n = 1.333$ and next nearest hopping $t' = 0.5$. We first show the phase diagram against on-site Coulomb interaction U and the nearest neighbor Coulomb interaction V (Fig. 2). There, we have assumed that the dominant superconductivity pairing is the one that has the largest eigenvalue λ in Eliashberg's equation calculated at $T = 0.03$. While the value of λ for $T = 0.03$ is still much smaller than unity, it is difficult to extend the FLEX calculation to lower temperatures, given the complexity of the (extended Hubbard) model. So this amounts to an assumption that the order in which λ 's appear for various pairing symmetries does not change for $T \rightarrow 0$. The charge density wave (CDW) is identified as the region in which the charge susceptibility (which has a peak at (π, π)) diverges at $T = 0.03$.

In the result a triplet superconductivity phase (which does not exist for a single band when V is absent) is seen to appear just below the CDW phase for $U > 9$. The maximum eigenvalue of charge and spin susceptibilities and detailed behavior of λ as a function of V for fixed $U = 10$ is shown in Fig. 3. From the figure we see that the triplet superconductivity becomes dominant when the charge susceptibility χ_{ch} is larger than the spin susceptibility χ_{sp} . Figure 4 shows gap functions in k -space, which shows that the triplet (which has

the highest λ) has a gap function $\propto \sin(k_x + k_y)$, while the two singlet gap functions have $\cos 2k_x - \cos 2k_y$ and $\sin k_x \sin k_y$.⁴²

We can trace back the reason why these gap functions are favored to the structure of spin and charge susceptibilities. Figure 5 shows the peak positions of spin and charge susceptibilities for $V = 2.7$. The peak positions for charge are around $(\pm\pi, \pm\pi)$, $(\pm\pi, \mp\pi)$, while those for spin are ferromagnetic-like around $(\pm\frac{\pi}{4}, \pm\frac{\pi}{4})$, $(\pm\frac{\pi}{4}, \mp\frac{\pi}{4})$. In Éliashberg's eq.(2)-(4), we see that for singlet the coefficient of χ_{sp} (χ_{ch}) term in Γ_s are positive (negative). So the dominant gap function must change sign across the momentum transfer that points the peak position in the spin susceptibility, while the gap function must not change sign across the momentum transfer that points the peak position in the charge susceptibility. For triplet, on the other hand, the coefficients of χ_{sp} and χ_{ch} terms in Γ_t are both negative. So the gap function should have the same sign across both the spin and charge peak positions.

When V is small, the spin susceptibility is much greater than the charge susceptibility, and the spin-fluctuation mediated pairing interaction for singlet is three times larger than that for triplet. This explains $\cos 2k_x - \cos 2k_y$, which changes sign across $(\pm\frac{\pi}{4}, \pm\frac{\pi}{4})$, $(\pm\frac{\pi}{4}, \mp\frac{\pi}{4})$, becomes the dominant gap function. For large V , the charge susceptibility becomes dominant, and the pairing interaction becomes the same between singlet and triplet channels, i.e., Γ_s and Γ_t become similar in magnitude. Whether triplet is more favored than singlet depends on the other factors such as the number of nodes on the Fermi surface, which work unfavorably for pairing since the integration around the node in the right hand side of eqn.(2) cannot contribute to λ . So a larger the number of nodes is basically unfavorable.

As another factor, we can find from Fig. 3 that the λ 's for the gap function $\sin(k_x + k_y)$ and $\sin k_x \sin k_y$ increase more sharply than that for $\cos 2k_x - \cos 2k_y$ for $V > 2$, where χ_{ch} increases sharply. The reason should be that the first two have the same sign across the peak of χ_{ch} around $(\pm\pi, \pm\pi)$ or $(\pm\pi, \mp\pi)$, while the latter has slightly warped nodal lines. So there is a region exists where the gap function has the opposite signs across the peak of χ_{ch} .

Returning to Sr_2RuO_4 , our result in Fig. 3 indicates that if triplet can be dominant, the gap function should be $\sin(k_x + k_y)$ which is degenerate with $\sin(k_x - k_y)$. The true gap function below T_c should be a complex linear combination,

$$\sin(k_x + k_y) + i \sin(k_x - k_y), \quad (10)$$

which is more stable thermodynamically and breaks the time-reversal symmetry (Fig. 6). The absolute value of the gap function has minima on the Fermi surface along [100] and equivalent directions as depicted in Fig. 6 with open circles, which is consistent with the recent experiment of the specific heat in rotated magnetic fields.¹³

However, we also notice that the triplet region is very narrow, so identification of the pairing in Sr_2RuO_4 would require a precise determination of the parameters in that material. In addition, if we include the effect of α and β band of Sr_2RuO_4 this triplet region may expand.

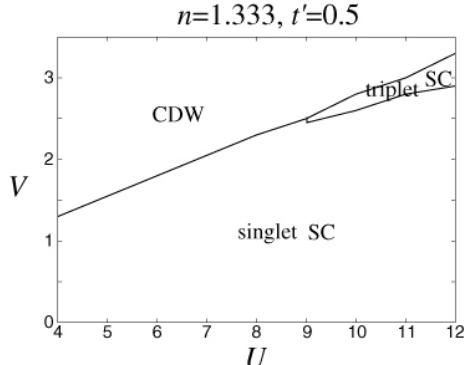


FIG. 2. Phase diagram against V and U with $n = 1.333$ and $t' = 0.5$ for the 2D extended Hubbard model.

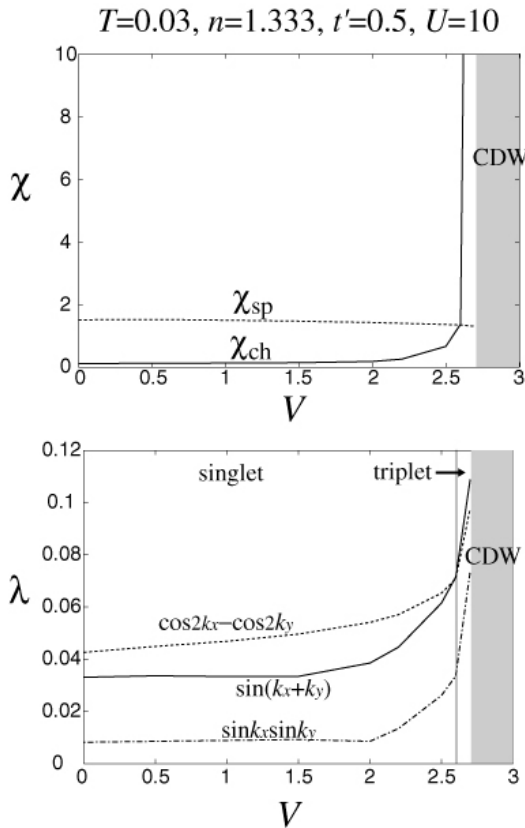


FIG. 3. Top: the maximum eigenvalue of $\chi_{\text{ch}}(\mathbf{k}, 0)$ charge (solid line) and $\chi_{\text{sp}}(\mathbf{k}, 0)$ spin (dotted) susceptibilities as a function of V for $U = 10.0$. Bottom: the eigenvalue λ of Éliashberg's equation for triplet $\sin(k_x + k_y)$ (solid line), singlet $\cos 2k_x - \cos 2k_y$ (dotted) and $\sin k_x + \sin k_y$ (dot-dash) as a function of V for $U = 10.0$. The CDW (gray) region is identified from the divergence in the charge susceptibility.

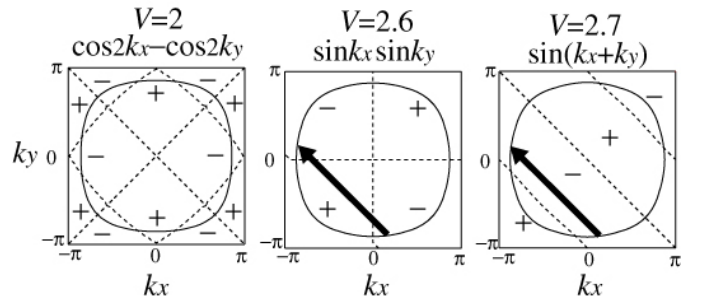


FIG. 4. The dominant gap function $\sin(k_x + k_y)$ (triplet) in k space for $V = 2.7$ (right panel), $\cos 2k_x - \cos 2k_y$ (singlet) for $V = 2$ (left), and sub-dominant singlet gap function $\sin k_x \sin k_y$ for $V = 2.6$ (center), each for $U = 10.0$. The arrows indicate the main scattering process mediated by charge fluctuation.

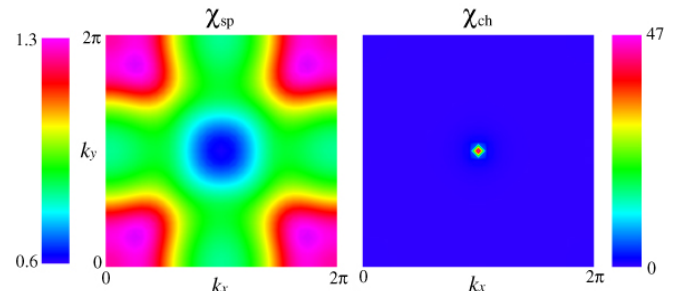


FIG. 5. Color-coded plots of the spin susceptibility $\chi_{\text{sp}}(\mathbf{k}, 0)$ (left) and the charge susceptibility $\chi_{\text{ch}}(\mathbf{k}, 0)$ (right) for $U = 10.0, V = 2.7$.

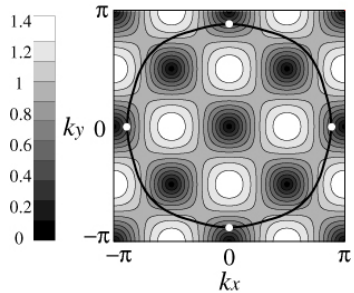


FIG. 6. Contour plot of $|\sin(k_x + k_y) + i \sin(k_x - k_y)|$ along with the Fermi surface for $T = 0.03, U = 10.0, V = 2.7$. Open circles indicate minima of the gap function on the Fermi surface.

B. Relation between the pairing symmetry and the Fermi surface

Let us identify the relation between the pairing symmetry and shape of the Fermi surface in the present con-

text. For that purpose we can change the second neighbor hopping t' , which controls the warping (and even the topology) of the Fermi surface. In Fig. 7 we show λ and the dominant pairing symmetry when t' is varied with fixed $U = 10.0$ and $V = 2.7$. Figure 8 depicts how the Fermi surface obtained by $\epsilon_{\mathbf{k}}^0 + \text{Re}\Sigma(k) = \mu$ changes with t' . The reason why those gap functions dominate can be understood in terms of the structure and value of the spin and charge susceptibilities. While the peaks in the spin susceptibility for $V = 0$ correspond to the nesting vectors for the Fermi surface, the peaks for large V do not necessarily correspond to those. The result shows that the peaks change from $(0.6\pi, \pi), (\pi, 0.6\pi)$ for $t' = 0 - 0.3$, $(0.3\pi, 0.3\pi)$ for $t' = 0.4 - 0.8$, to $(0, 0.5\pi), (\pi, 0.5\pi)$ for $t' = 0.9 - 1.0$ as seen in Fig. 9. On the other hand the peak position in the charge susceptibility remains at (π, π) for the whole range of t' . The peak values of $\chi_{\text{ch}}(\mathbf{k}, 0)$ and $\chi_{\text{sp}}(\mathbf{k}, 0)$ are shown in Fig. 10, where the peak of $\chi_{\text{ch}}(\mathbf{k}, 0)$ changes rapidly while $\chi_{\text{sp}}(\mathbf{k}, 0)$ has an almost constant peak value.

From the result we see that nearly antiferromagnetic spin fluctuations favor $d_{x^2-y^2}$ pairing for $t' = 0 - 0.3$ as in the high- T_c cuprates, strong charge fluctuations favor $\sin(k_x + k_y)$ for $t' = 0.3 - 0.6$. For $t' = 0.7 - 1.0$ where the spin susceptibility again exceeds the charge susceptibility, nearly ferromagnetic spin fluctuations favor $\cos 2k_x - \cos 2k_y$ which has many sign changes on the Fermi surface.

Finally it is interesting to identify the reason why the charge fluctuation is sharply peaked around $t' = 0.4$. To elaborate the point, we first note the van-Hove singularities, which reside at $(0, \pm\pi), (\pm\pi, 0), (\pm \arccos(-t/(2t')), \pm \arccos(-t/(2t')))$ and $(\pm \arccos(-t/(2t')), \mp \arccos(-t/(2t')))$ for the $t - t'$ tight-binding model. So the charge susceptibility with a peak around (π, π) should be maximized when the Fermi surface approaches $(0, \pm\pi)$ and $(\pm\pi, 0)$, since the pair hopping with the momentum transfer (π, π) connects the van-Hove singularities, where the density of state is large. In the terminology of the previous work of ours⁴³, the Fermi surface becomes “thick” around the van-Hove singularities.

We have actually studied the relation between the charge susceptibility and the Fermi surface as shown in Fig. 11 to confirm that the charge susceptibility becomes maximum for $t' = 0.41$, at which the Fermi surface just touches the van-Hove singularities $(0, \pm\pi), (\pm\pi, 0)$ and the topology of the Fermi surface changes. We see in the figure that the Fermi surface becomes “thick” around the van-Hove singularities. The value $t' = 0.4$ is close to the t' for γ band of Sr_2RuO_4 , which may imply that triplet superconductivity induced by charge fluctuations may in fact be relevant there.

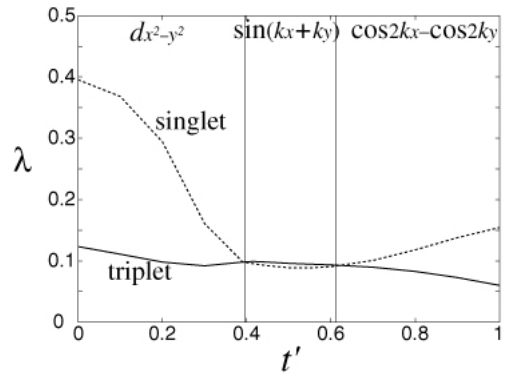


FIG. 7. The maximum eigenvalue λ of Éliashberg’s equation for spin-triplet (solid line), spin-singlet (dotted) as a function of the second neighbor hopping t' for $U = 10.0$ and $V = 2.7$ with the dominant pairing symmetry indicated

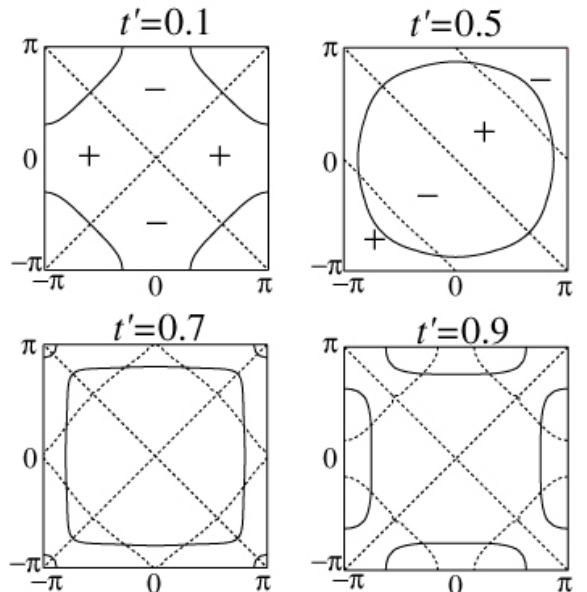


FIG. 8. Fermi surface (solid line) and nodes of the dominant gap function (dotted) for $t' = 0.1$ (top left), $t' = 0.5$ (top right), $t' = 0.7$ (bottom left) and $t' = 0.9$ (bottom right) for $U = 10.0$ and $V = 2.7$.

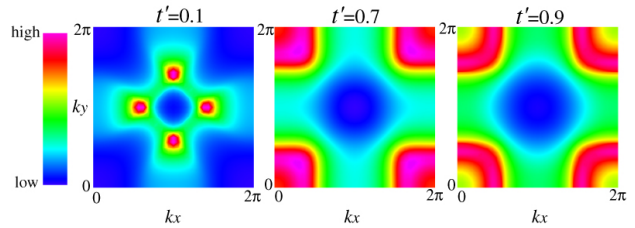


FIG. 9. Color-coded plots of the spin susceptibility $\chi_{\text{sp}}(\mathbf{k}, 0)$ for $t' = 0.1$ (left), $t' = 0.7$ (center), and $t' = 0.9$ (right) for $U = 10.0$ and $V = 2.7$.

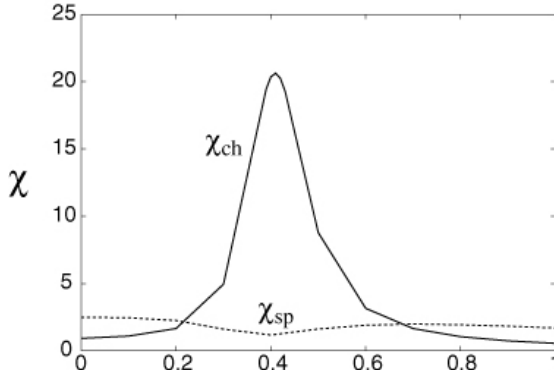


FIG. 10. The maximum eigenvalue of $\chi_{\text{ch}}(\mathbf{k}, 0)$ (solid line) and $\chi_{\text{sp}}(\mathbf{k}, 0)$ (dotted) as a function of t' for $U = 10.0$ and $V = 2.7$.

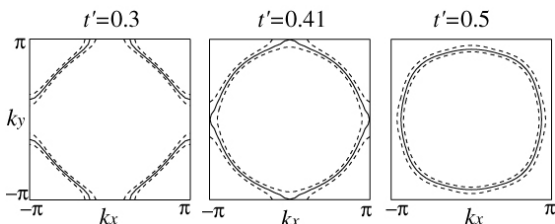


FIG. 11. The t' dependence of the Fermi surface (solid lines), while dotted lines delineate $E = E_F \pm 0.2$ for $U = 10.0$, $V = 2.7$.

C. Real-space representation

So far we have shown all the results in \mathbf{k} -space, but it is also heuristic to represent the pairing symmetry in real space as depicted in Fig. 12. From Fig. 7-10 we see that $d_{x^2-y^2}$ is suppressed as the (π, π) charge fluctuation increases, while from Fig. 3 $\sin(k_x + k_y)$, d_{xy} and $\cos 2k_x - \cos 2k_y$ are favored as the charge fluctuation increases. This should be because strong (π, π) charge fluctuations tend to arrange electrons diagonally on the lattice, and suppresses $d_{x^2-y^2}$ pairs across the nearest neighbors, but do not disturb the pairing such as $\sin(k_x + k_y)$, d_{xy} and $\cos 2k_x - \cos 2k_y$ formed across more distant sites.

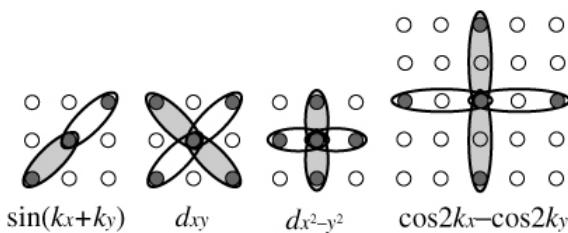


FIG. 12. The pairing symmetry in real space.

IV. CONCLUSION

We have studied the pairing symmetry in the one-band extended Hubbard model having the nearest neighbor Coulomb repulsion for square lattice. For the parameter which represents γ band of Sr_2RuO_4 , spin-triplet superconductivity whose symmetry is $\sin(k_x + k_y)$ appears just below the CDW phase. So the true gap below T_c is suggested to be a chiral $\sin(k_x + k_y) + i \sin(k_x - k_y)$ which breaks the time-reversal symmetry. However, the region for the spin-triplet superconductivity is very small, and the identification of the pairing in Sr_2RuO_4 will require a precise determination of parameters, and also a study of the effects of α and β bands.

We have also examined the relation between the pairing symmetry and the shape of the Fermi surface by varying t' . As t' increases, the shape of the Fermi surface changes drastically which changes the structure of χ_{sp} and χ_{ch} . This in turn changes the pairing symmetry as $d_{x^2-y^2} \rightarrow \sin(k_x + k_y) \rightarrow \cos 2k_x - \cos 2k_y$. In addition, χ_{ch} becomes especially large when the Fermi surface touches van-Hove singularities at which the Fermi surface changes the topology, which is achieved for $t' = 0.41$ near the parameter for γ band of Sr_2RuO_4 .

V. ACKNOWLEDGMENTS

Numerical calculations were performed at the supercomputer center, ISSP.

* Present address: Graduate School of Engineering, Nagoya University, Chikusa, Nagoya 464-8603, Japan.

- ¹ R. Arita, K. Kuroki, and H. Aoki, Phys. Rev. B **60**, 14585 (1999); J. Phys. Soc. Jpn. **69**, 1181 (2000).
- ² P. Monthoux and G. Lonzarich, Phys. Rev. B **59**, 14598 (1999).
- ³ K. Ishida, H. Mukuda, Y. Kitaoka, K. Asayama, Z. Q. Mao, Y. Mori, and Y. Maeno, Nature (London) **396**, 658 (1998).
- ⁴ K. Ishida, H. Mukuda, Y. Kitaoka, Z. Q. Mao, H. Fukazawa, and Y. Maeno, Phys. Rev. B **63**, 060507(R) (2001).
- ⁵ J. A. Duffy, S. M. Hyden, Y. Maeno, Z. Mao, J. Kulda, and G. J. McIntyre, Phys. Rev. Lett. **85**, 5412 (2000).
- ⁶ G. M. Luke, Y. Fudamoto, K. M. Kojima, M. I. Larkin, J. Merrin, B. Nachumi, Y. J. Uemura, Y. Maeno, Z. Q. Mao, Y. Mori, H. Nakamura, and M. Sigrist, Nature (London) **394**, 448 (1998).
- ⁷ G. M. Luke, Y. Fudamoto, K. M. Kojima, M. I. Larkin, B. Nachumi, Y. J. Uemura, J. E. Sonier, Y. Maeno, Z. Q. Mao, Y. Mori, H. Nakamura, and D. Agterberg, Physica B **289**, 373 (2000).

⁸ P. G. Kealey, T. M. Riseman, E. M. Forgan, A. P. Mackenzie, L. M. Galvin, S. L. Lee, D. McK. Paul, R. Cubitt, D. F. Agterberg, R. Heeb, Z. Q. Mao, and Y. Maeno, Phys. Rev. Lett. **84**, 6094 (2000).

⁹ K. Ishida, Y. Kitaoka, K. Asayama, S. Ikeda, S. Nishizaki, Y. Maeno, K. Yoshida, and T. Fujita, Phys. Rev. B **56**, R505 (1997).

¹⁰ K. Ishida, H. Mukuda, Y. Kitaoka, Z. Q. Mao, H. Fukazawa, and Y. Maeno, Phys. Rev. Lett. **84**, 5387 (2000).

¹¹ S. NishiZaki, Y. Maeno, and Z. Q. Mao, J. Phys. Soc. Jpn. **69**, 572 (2000).

¹² K. Izawa, H. Takahashi, H. Yamaguchi, Y. Matsuda, M. Suzuki, T. Sasaki, T. Fukase, Y. Yoshida, R. Settai, and Y. Onuki, Phys. Rev. Lett. **86**, 2653 (2001).

¹³ K. Deguchi, Z. Q. Mao, H. Yaguchi, and Y. Maeno, Phys. Rev. Lett. **92**, 047002 (2004).

¹⁴ M. E. Zhitomirsky and T. M. Rice, Phys. Rev. Lett. **87**, 057001 (2001).

¹⁵ T. Kuwabara and M. Ogata, Phys. Rev. Lett. **85**, 4586 (2000).

¹⁶ M. Sato and M. Kohmoto, J. Phys. Soc. Jpn. **69**, 3505 (2000).

¹⁷ K. Miyake and O. Narikiyo, Phys. Rev. Lett. **83**, 1423 (1999).

¹⁸ T. Nomura and K. Yamada, J. Phys. Soc. Jpn. **69**, 3678 (2000).

¹⁹ T. Nomura and K. Yamada, J. Phys. Soc. Jpn. **71**, 1993 (2002).

²⁰ Y. Yanase and M. Ogata, J. Phys. Soc. Jpn. **72**, 473 (2003).

²¹ K. Kuroki, M. Ogata, R. Arita, and H. Aoki, Phys. Rev. B **63**, 060506 (2001).

²² K. Kuroki, Y. Tanaka, T. Kimura, and R. Arita, Phys. Rev. B **69**, 214511 (2004).

²³ R. Arita, S. Onari, K. Kuroki, and H. Aoki, Phys. Rev. Lett. **92**, 247006 (2004).

²⁴ S. Onari, R. Arita, K. Kuroki, and H. Aoki, Phys. Rev. B **70**, 094523 (2004).

²⁵ Y. Zhang and J. Callaway, Phys. Rev. B **39**, 9397 (1989).

²⁶ Z. Tešanović, A. R. Bishop, and R. L. Martin, Solid State Commun. **68**, 337 (1988).

²⁷ M. Murakami, J. Phys. Soc. Jpn. **69**, 1113 (2000).

²⁸ H. Seo and H. Fukuyama, J. Phys. Soc. Jpn. **66**, 1249 (1997).

²⁹ M. Onozawa, Y. Fukumoto, A. Oguchi, and Y. Mizuno, Phys. Rev. B **62**, 9648 (2000).

³⁰ D. J. Scalapino, E. Loh, Jr., and J. E. Hirsch, Phys. Rev. B **35**, 6694 (1987).

³¹ G. Esirgen, H.B. Schuttler, and N. E. Bickers, Phys. Rev. Lett. **82**, 1217 (1999).

³² J. Merino and R. H. McKenzie, Phys. Rev. Lett. **87**, 237002 (2001).

³³ K. Sano and Y. Ono, J. Phys. Chem. Solids **63**, 1567 (2002).

³⁴ K. Kuroki, K. Kusakabe, and H. Aoki, Phys. Rev. B **50**, 575 (1994).

³⁵ N. E. Bickers, D. J. Scalapino, and S.R. White, Phys. Rev. Lett. **62**, 961 (1989).

³⁶ N. E. Bickers and D. J. Scalapino, Ann. Phys. (N.Y.) **193**, 206 (1989).

³⁷ T. Dahm and L. Tewordt, Phys. Rev. B **52**, 1297 (1995).

³⁸ M. Langer, J. Schmalian, S. Grabowski, and K. H. Bennemann, Phys. Rev. Lett. **75**, 4508 (1995).

³⁹ G. Esirgen and N. E. Bickers, Phys. Rev. B **55**, 2122 (1997).

⁴⁰ G. Esirgen and N. E. Bickers, Phys. Rev. B **57**, 5376 (1998).

⁴¹ A. Damascelli, *et al.*, Phys. Rev. Lett. **85**, 5194 (2000).

⁴² In Ref.²² the dominant spin singlet gap function is $d_{x^2-y^2}$ for $U = 4$, $t' = 0.4$ with $V = 0$, where the spin structure is antiferromagnetic (peaked at $(\pi, \pi/2)$), but our result for $t' = 0.5$ has a ferromagnetic-like spin susceptibility which suppresses $d_{x^2-y^2}$.

⁴³ S. Onari, R. Arita, K. Kuroki, and H. Aoki, Phys. Rev. B **68**, 024525 (2003).